The Role of Microstructure in Hydrogen-Assisted Fracture of 7075 Aluminum

J. ALBRECHT, A. W. THOMPSON, AND I. M. BERNSTEIN

Underaged, peak strength (T6), and overaged (T73) microstructures were studied in 7075 plate material. Hydrogen charged and uncharged tensile specimens of longitudinal orientation were tested between −196°C and room temperature. The results confirm a hydrogen embrittlement effect, manifested mainly in the temperature dependence of the reduction of area loss; a classical behavior of hydrogen embrittlement. The maximum embrittlement shifted to lower temperatures with further aging. The effect of hydrogen was largest for the underaged condition and smallest for the overaged, thus following the pattern found for the sensitivity to stress-corrosion cracking in high strength aluminum alloys. The fracture path was predominantly transgranular, with minor amounts of intergranular fracture.

WHILE the resistance of high strength aluminum alloys to environmentally assisted fracture long has been a subject of considerable practical concern, fundamental studies of this problem have usually not been sufficiently detailed to identify the underlying process of fracture (for example, whether fracture is controlled by anodic dissolution, hydrogen embrittlement, or some combination of both). Even less understanding exists as to why this type of fracture is sensitive to metallurgical variables, such as composition,[1-3] microstructure,[2,3] grain shape and texture,[2,4,5] and thermal treatment.[2,3] The microstructure variable is of particular interest, since this is the variable that can be manipulated in a given alloy over a considerable range while maintaining the composition, grain shape, and texture developed from the alloy's processing history.

The microstructural variable that is thought to be of primary importance in the environmental fracture behavior of aluminum alloys is the character (nature and distribution) of the precipitate population.[6,7] The influence of precipitates both in the grain interior and at grain boundaries can be explained by two behavior features: i) The character of those grain interior precipitates which control slip mode by whether or not they are sheared during deformation; when sheared, planar slip results, with accompanying low resistance to stress corrosion cracking (SCC), while if they are not sheared, slip is wavy and SCC resistance tends to be higher;[6,8] ii) The relative coverage of grain boundaries by the intergranular precipitates. An increased coverage has been correlated with SCC resistance.[6,9] Unfortunately, these two behavioral features are difficult to separate experimentally because thermal treatments which change the grain interior precipitates also in general affect grain boundary precipitates. Mechanistically, it now appears[6,7] that both features play a role in SCC susceptibility.

It has been proposed[6] that slip planarity may be important to SCC processes because of its importance to hydrogen* transport,[10] while the grain boundary precipitates might be independently important as accumulators of hydrogen* and thus potential nuclei for localized fracture.[6,7,13-15] One way to separate these phenomena is to deliberately use a specimen orientation which is not subject to significant intergranular fracture. In SCC testing, the longitudinal orientation in plate or bar products would be appropriate.[2] It may still be true, however, that the relative planarity of slip could affect both the processes of anodic dissolution and hydrogen embrittlement. A way to further separate these contributions is to study the role of planarity in a single process; *i.e.*, under conditions where only hydrogen is present. Accordingly, the present work has emphasized behavior of hydrogen charged longitudinal specimens.

We have recently shown[16] that 7075-T651 bar material exhibits significant losses in ductility when cathodically charged with hydrogen; those results reproduced fairly closely those obtained by Gest and Troiano.[17,18] Similar experimental techniques were employed in the work described here, except that 7075 plate material was used instead of bar material.

*Here we accept the view that hydrogen embrittlement processes contribute to SCC of aluminum alloys.[6,7,11,12]

EXPERIMENTAL PROCEDURE

The material used was commercial 7075 plate material, 63.5 mm thick, with the composition listed in Table I. This plate is part of a heat that has been extensively studied at Alcoa Laboratories (identification no. 420436) and was supplied to us by them. The grain structure of the plate, as shown in Fig. 1, is the disk shaped (sometimes called "pancake") arrangement typical of commercial product.[2] Tensile specimens with 5.3 mm diam and 25 mm gage length were cut from the plate with the tensile axis parallel to the longitudinal direction (RD in Fig. 1),* and polished mechanically after machining to give a uniform surface finish. Polishing was performed with 600 grit paper followed by oil based Linde B compound to minimize exposure to water.

*A few specimens were cut at 45 deg to RD with the tensile axis lying in the RD-ST plane for special experiments.

J. ALBRECHT, formerly with the Department of Metallurgy and Materials Science, Carnegie-Mellon University, is now with Brown-Boveri Research Center, CH 5401, Baden, Switzerland. A. W. THOMPSON and I. M. BERNSTEIN are Professors, Department of Metallurgy and Materials Science, Carnegie-Mellon University, Pittsburgh, PA, 15213.

Manuscript submitted December 5, 1978.

ISSN 0360-2133/79/1112-1759$00.75/0

Table I. Composition of 7075 Plate Material*, Wt Pct

Zn	Mg	Cu	Cr	Fe	Si	Mn	Ti	Be
5.68	2.48	1.63	0.19	0.30	0.12	0.07	0.05	0.001

*Alcoa Laboratories no. 420436; conforms to QQA-250/12d specifications; plate center electrical conductivity in T651 condition is 33.2 pct IACS.

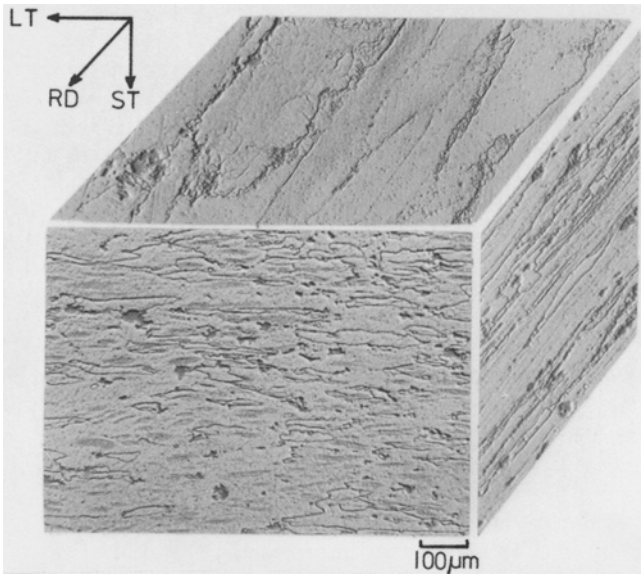

Fig. 1—Grain morphology of the 7075 plate material (light micrograph) relative to the rolling direction (RD) and transverse directions.

Specimens were then given a conventional solution treatment in a salt bath; 20 min at 465°C, followed by quenching into ice water. This solution treatment not only dissolved existing precipitates, but also annealed any mechanically deformed surface layer resulting from machining and polishing. This procedure is important, since a high dislocation density in near-surface regions could affect both hydrogen permeability and transport of hydrogen by mobile dislocations.[19-21]

After quenching, the specimens were pre-aged for a minimum of 50 h at room temperature to optimize mechanical properties.[22] During this time, the samples were electropolished in a perchloric-ethanol solution at −30°C. The final aging treatment used was one of the following: T6 (peak-aged temper; 24 h at 120°C), T73 temper (overaged, 24 h at 163°C), and an underaging treatment called UT (24 h at 100°C) designed to give about the same room temperature yield strength as the T73 treatment. Specimens for hydrogen testing were cathodically charged in a hydrochloric acid solution (pH = 1), for 10 h under an applied constant potential of −1500 mV *vs* standard calomel electrode. The 10 h time was chosen for convenience, since hydrogen effects did not vary for times between 5 and 24 h. After charging, the specimens were rinsed with water, dried, and stored in liquid nitrogen to reduce the loss of internal hydrogen.

In earlier work,[16] it was found that appreciable intergranular corrosion occurred during hydrogen charging. In the present work, two aspects of specimen preparation were changed in order to prevent such attack. Specifically, the near-surface deformed layer was annealed prior to charging, as described above, and chemical polishing[17,18] was omitted. The new procedure resulted in no detectable corrosion penetration (<1 μm), as observed in longitudinal sections of the charged material.

Tensile tests were performed at an initial strain rate of $\dot{\epsilon} = 8.3 \times 10^{-4}\ s^{-1}$. Charged and uncharged (reference) specimens were tested at temperatures of −196, −98, −50, and 20°C. Temperature control during testing was maintained by submerging each tensile sample and the grips either in liquid nitrogen or in a suitable two-phase bath. Reference mechanical properties are shown in Table II. To calculate the fracture strain, the diameter of the necked region was measured using a measuring microscope with a resolution of 1 μm. To assess experimental scatter, at least three samples were tested for each condition.

Transmission electron microscopy examination of thin foils of each of the microstructures was performed; foils were prepared using standard electropolishing conditions in a 1:2 nitric acid-methanol electrolyte.[23] Phase identification in these foils was accomplished by electron diffraction methods.[1] Fracture surfaces of broken tensile specimens were examined using a scanning electron microscope (SEM).

RESULTS

The grain structure of the plate material is shown in Fig. 1; it is typical of hot-rolled aluminum alloy plate, with the grain size approximately 400 μm in the longitudinal direction, 100 to 200 μm in the long transverse direction, and approximately 50 μm in the short transverse direction. Large inclusions containing the impurity elements iron and silicon are found primarily at grain boundaries (these appear as black dots in Fig. 1).

Details of the microstructure[1] for the different heat treatments are shown in Fig. 2. Independent of aging conditions, the material contains fine, chromium-rich intermetallic particles, which are not dissolved during the solution heat treatment. In the 7000 series alloys, chromium is added to form these intermetallic particles, mainly for purposes of grain refinement.[2] The size of these incoherent particles is about 0.2 to 0.5 μm.

In the underaged or UT condition (Fig. 2(*a*)) the matrix contains fine, homogeneously distributed

Table II. Mechanical Properties of Experimental Materials (in the absence of hydrogen)

Test Temp., °C	Condition	Yield Strength,* MPa	Ultimate Tensile Strength, MPa	Reduction of Area, Pct
20	UT	427	537	27
	T6	489	571	29
	T73	441	517	33
−98	UT	489	600	22
	T6	544	607	23
	T73	482	585	26
−196	UT	544	655	17
	T6	586	655	19
	T73	517	614	21

*Flow stress at plastic strain of 0.002.

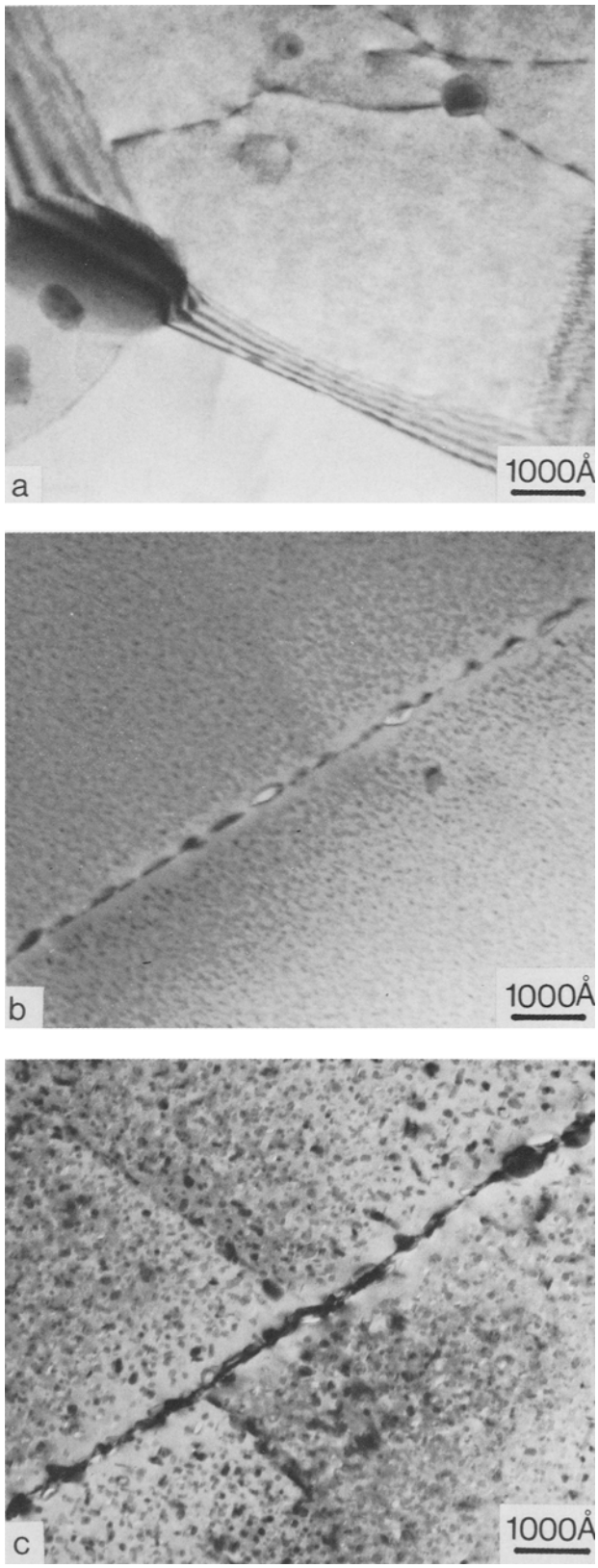

Fig. 2—Transmission electron micrographs of microstructural details of the three heat treatments: (*a*) underaged, UT, (*b*) T6, (*c*) T73.

coherent precipitates (GP zones) with a size of approximately 15 to 20Å. In the peak-aged condition (T6, Fig. 2(*b*)) a mixture of GP zones and the semi-coherent intermediate phase (usually called η') is precipitated within the matrix. In addition, the equilibrium η ($MgZn_2$) phase is precipitated at the grain boundaries as incoherent particles; this is accompanied by the formation of a precipitate-free zone along the grain boundaries with a width of 250Å.

In the overaged condition (T73, Fig. 2(*c*)), the matrix contains relatively coarse η' particles; the grain boundaries are covered by large η particles as well as even larger T-phase, $(Al\ Zn)_{49}\ Mg_{32}$, particles. The width of the precipitate-free zone in this condition is about 350Å.

The results of tensile tests on the above materials are shown in Fig. 3. Plotted is the reduction of area (RA) *vs* test temperature for both charged and uncharged specimens for the underaged condition (Fig. 3(*a*)), for T6 (Fig. 3(*b*)) and for T73 (Fig. 3(*c*)). At temperatures above −100°C, the RA loss* due to hydrogen charging is largest for the underaged condition, smallest for the overaged material, and intermediate for the peak-aged T6 condition, while at −196°C, no significant effect of hydrogen was found for any condition. The RA loss data for the charged specimens as a function of temperature are shown in Fig. 4. They exhibit distinct maxima for the overaged material at around −100°C, for the T6 temper in the range of −50°C, and for the underaged condition near room temperature.

* Defined as $(RA\text{-}RA_{hydrogen}) \div RA$.

Examination of the fracture surfaces showed that the fracture path was mainly transgranular, independent of microstructure, test temperature, and charging condition. Figure 5 shows details of the fracture surfaces for the room temperature tests for charged and uncharged specimens of the UT, T6, and T73 conditions. In all cases, both small and large dimples were found. The size and distribution of the small dimples corresponds to the chromium rich dispersoids, whereas the large dimples can be associated with the large impurity inclusions. A small amount (less than 10 pct) of intergranular fracture was found, the extent of which varied slightly with test temperature, being greatest for the T73 temper. The persistent occurrence of transgranular fracture is believed due to the disk shaped grain structure. With the tensile axis parallel to the rolling direction, the major part of the grain boundary area is parallel to the load axis. Even though grain boundary fracture is favored due to the presence of soft, precipitate-free zones in the T6 and T73 tempers, the stress on the grain boundaries for this specimen orientation is not high enough to fracture the boundaries.[2]

At low test temperatures (−50 to −200°C), secondary cracks were found. Examples of these cracks can be seen on the T6 fracture surfaces at −196°C, for both the charged and uncharged condition (Fig. 6). The effect of secondary cracking, however, is not as pronounced as in the 7075 bar material tested previously.[16] By sectioning fractured specimens parallel to the tensile axis and then polishing and etching (Fig. 7) it was shown that these secondary cracks lie in grain boundaries parallel to the rolling direction (see Fig. 1).

As a test of the foregoing comments, specimens with tensile axes at 45 deg to the RD in the RD-ST plane were heat treated to the T6 temper and tested at room temperature in both hydrogen charged and uncharged conditions. The fracture path was found to be almost

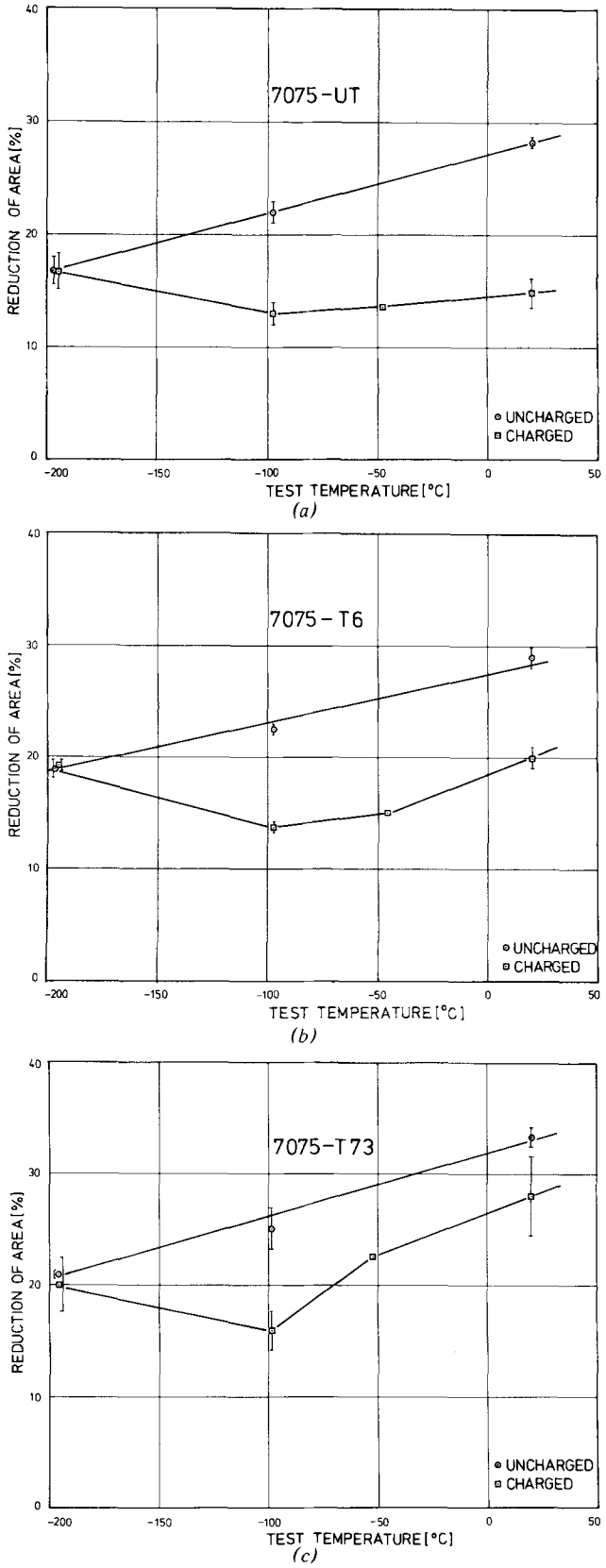

Fig. 3—Results of the tensile tests: Reduction of area *vs* test temperature: (*a*) underaged (UT), (*b*) T6, (*c*) T73.

exclusively intergranular, as shown in Fig. 8. The grain boundaries are fairly smooth with *shallow* dimples (Fig. 8(*a*)), as would be expected for a shear type intergranular fracture, while transgranular tearing across a few grains produced occasional dimpled steps (Fig. 8(*b*)).

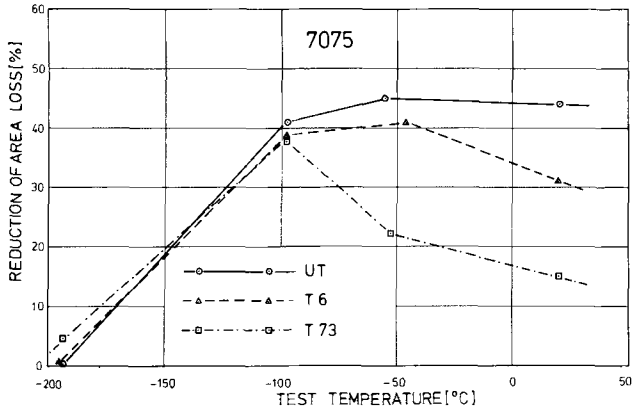

Fig. 4—Reduction of area loss *vs* test temperature for the three different microstructures.

The dimpled fracture areas of one specimen of each microstructure, test temperature and hydrogen content were photographed using an SEM, with the tensile axis accurately aligned with the viewing direction. The specimens chosen were those whose RA value was closest to the mean value for each condition. The diameters of 100 dimples in a typical area about 500 μm from the gage surface were measured in each case. Results are shown in Table III. None of the differences are significant at −196°C, but above that temperature, in the UT condition, dimple sizes are significantly increased by hydrogen, while in the T73 condition the size is significantly decreased. For T6 material, the dimple size did not change significantly.

DISCUSSION

The results reported above, in combination with earlier reports,[16-18] clearly show that cathodically charged hydrogen reduces the ductility of 7075 aluminum. As is typical of hydrogen embrittlement,[24] the temperature dependence, Fig. 3, shows a distinct maximum as a function of temperature; moreover, the effect is absent at −196°C, ruling out a purely mechanical effect due, for example, to some kind of charging damage present prior to mechanical testing.

The principal new finding of this work is that the ductility loss is a function of microstructure. This effect was largest for the underaged microstructure and smallest for the overaged, suggesting that the degree of susceptibility to hydrogen embrittlement is strongly correlated to slip planarity.[7] In the underaged condition used here, with yield strength about 10 pct less than for T6, the coherent GP zones present in the matrix can be cut by passing dislocations, leading to a local softening of the slip plane and thus to the formation of concentrated slip bands.[25] In the T73 temper, the matrix precipitates are semicoherent, resulting in a homogeneous slip distribution.[25] The T6 temper represents a transition state; the matrix contains a mixture of GP zones and semicoherent η' precipitates. In this condition, the slip distribution is inhomogeneous at low plastic strain, but with increasing strain becomes more and more homogeneous.[25] The correlation between slip distribution and hydrogen sensitivity suggests the possibility that hydrogen transport in this material is importantly influenced by mobile dislocations.[26,27] With the low hydrogen diffu-

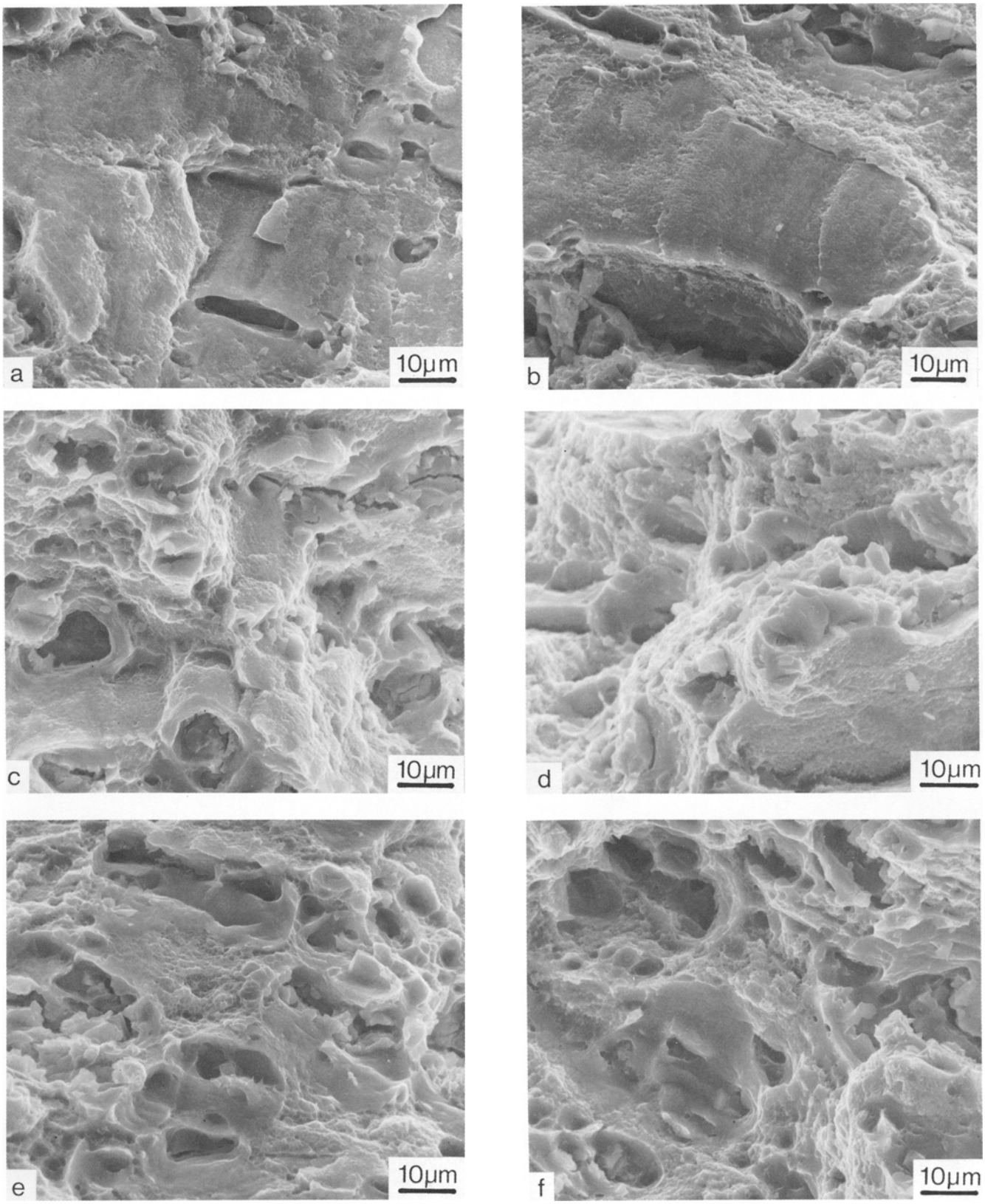

Fig. 5—Typical fracture surfaces (SEM), test temperature 20°C: (*a*) underaged, uncharged, (*b*) underaged, charged, (*c*) T6, uncharged, (*d*) T6, charged, (*e*) T73, uncharged, (*f*) T73, charged.

sivity[28] in aluminum the large embrittling effect of hydrogen appears difficult to explain by lattice diffusion; several accelerative mechanisms have been suggested,[26,29] including the dislocation transport of hydrogen as condensed atmospheres. Our findings support the possibility of a dislocation transport mechanism. We believe, as do many others, that a certain, critical hydrogen concentration is needed locally to cause macroscopic embrittlement. The accumulation of this critical amount of hydrogen should

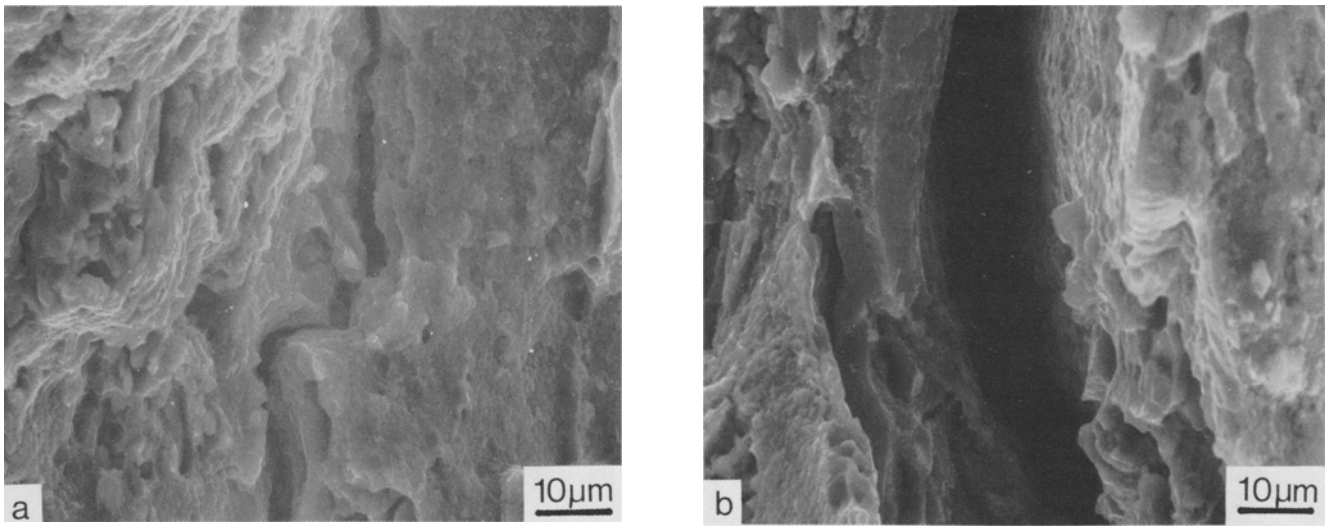

Fig. 6–Typical fracture surfaces (SEM) at 196°C: (*a*) T6, uncharged, (*b*) T6, charged.

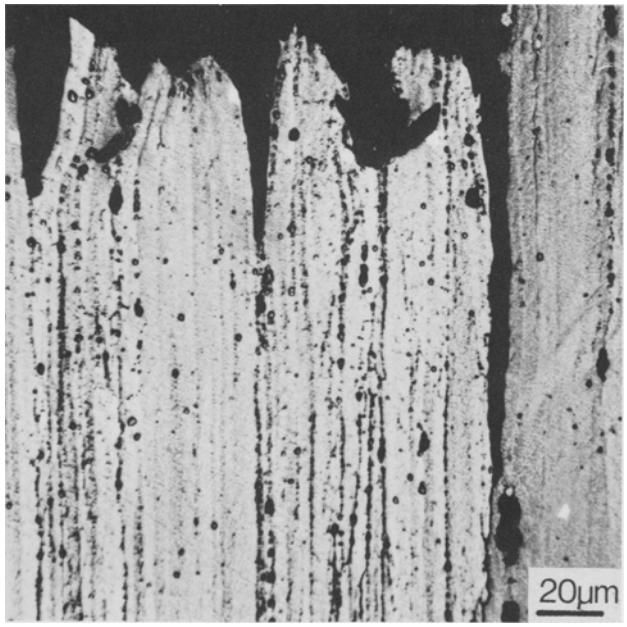

Fig. 7–Intergranular secondary cracking (light micrograph); T6, charged, tested at −196°C.

Table III. Fracture Surface Dimple Size* for the Three Microstructures at Three Test Temperatures

Material		Test Temperature −196°C	−98°C	20°C
UT	uncharged	0.142 ± 0.041	0.160 ± 0.049¶	0.156 ± 0.054
	H charged	0.166 ± 0.067	0.195 ± 0.063	0.178 ± 0.073†
T6	uncharged	0.161 ± 0.059	0.143 ± 0.040	0.196 ± 0.060
	H charged	0.138 ± 0.041	0.148 ± 0.049	0.183 ± 0.064
T73	uncharged	0.123 ± 0.038	0.185 ± 0.053¶	0.205 ± 0.060
	H charged	0.128 ± 0.037	0.110 ± 0.038	0.178 ± 0.045¶

*Values shown are dimple diameters in μm, ± standard deviation (1σ).
†Difference in mean values significant at 95 pct level.
¶Difference in mean values significant at 99 pct level.

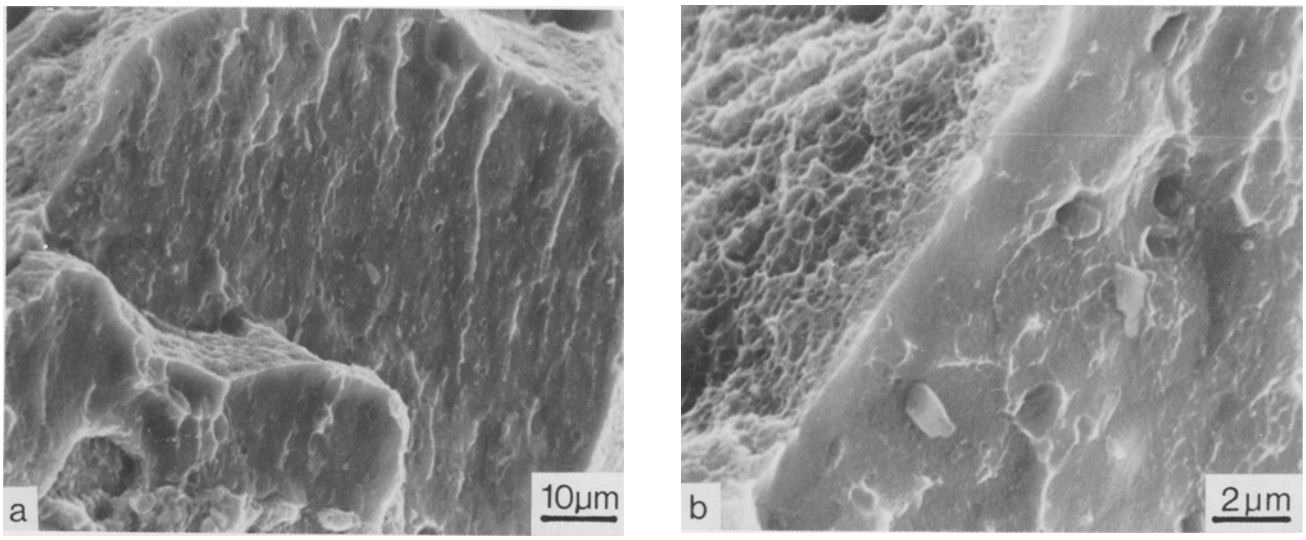

Fig. 8–Fracture surface (SEM) of a specimen cut 45 deg to the rolling direction; T6, test temperature 20°C: (*a*) Intergranular, shear type fracture, (*b*) Small amounts of transgranular, dimple type fracture.

be favored by an inhomogeneous slip distribution. With a homogeneous distribution of dislocations the overall hydrogen concentration might be the same, but the critical hydrogen concentration to cause embrittlement would not be reached locally.

This leads directly to the question as to the nature of the sites at which hydrogen is transported and accumulated.[7] It is known that hydrogen is accumulated at grain boundaries,[30-32] as well as precipitates, dispersoids and pores.[7,15,26] Since the fracture mode is transgranular, even in the presence of hydrogen, the RA loss is apparently not caused by embrittlement of the grain boundaries, suggesting that the other sites mentioned could serve as nuclei for the observed dimpled fracture. To address this question, we carried out a statistical analysis of dimple diameters on the fracture surface[33,34] as a function of heat treatment, charging condition and test temperature; the results of the analysis are shown in Table III.

These data show statistically significant changes in dimple diameter (above −196°C) only for the UT and T73 conditions, but the total cross-section of the embrittled specimens is in every case significantly larger (lower RA) than for the uncharged material. Thus for each condition, UT, T6, and T73, it is necessary to compare the observed dimple size ratio, (dimple diameter)$_H$ ÷ (dimple diameter), to that predicted geometrically from the RA change alone.[34] When this is done, both the T6 and T73 data (above −196°C) in Table III indicate that the total number of dimples is higher in the charged specimens, which can most simply be explained by enhanced nucleation of microvoids due to hydrogen.[33-36] This is consistent with the presence of semicoherent and incoherent precipitates in the T6 and T73 conditions, which may act as additional fracture nuclei in hydrogen charged specimens. On the other hand, dimple sizes are increased beyond the geometrical prediction[34] in UT specimens, indicating that the effect of hydrogen is primarily on microvoid growth.[33,34,36] This would be consistent with the relatively planar slip and relatively few additional fracture nuclei available in this condition.[33] Further experiments will be necessary to investigate the role of dislocations and to obtain more detailed information about hydrogen accumulation sites and the process of fracture nucleation.

It is important to recognize that the transgranular fractures observed in the present tests on longitudinal specimens are different from the intergranular fractures normally observed in SCC of short transverse specimens of commercial plate product.[2] Nevertheless, the T73 condition was more resistant to hydrogen, in contrast to the conclusion drawn from a corrosion fatigue study,[37] that overaging is only beneficial to environmentally assisted fracture when an intergranular fracture mode is observed. The lack of improvement from T73 aging in that work[37] must have arisen from some other cause than fracture path.

The work of Swann, Scamans and coworkers[30-32] has clearly shown that the presence of hydrogen can damage grain boundaries in high purity Al-Zn-Mg alloys with equiaxed grain structure; they also showed that addition of 1.7 pct Cu (see Table I) greatly increased resistance to hydrogen effects. Thus, it is unclear that the well known benefits of Cu to SCC resistance[2,6,7] of these alloys is in fact electrochemical in nature, as has been claimed.[38] The role of grain boundary microchemistry changes, particularly Mg segregation,[39] is also unclear, but the pronounced Mg-H interaction which would be expected[15] may well be part of any explanation of hydrogen effects in these alloys.

The transgranular fractures in the present work evidently stem from the orientation of the tensile axis relative to the major grain boundary surfaces. Even if the grain boundaries were embrittled by hydrogen, or softened by the formation of precipitate-free zones, neither the shear stress nor the normal stress is evidently high enough to fracture the grain boundaries. It was to test this possibility that the 45 deg specimens were used; in such an orientation, the shear stress on the major grain boundary surfaces is maximized and the normal stress on the boundaries is minimized. As Fig. 8 shows, intergranular fractures were observed and a hydrogen induced ductility loss was present. The secondary cracking observations in the longitudinal specimens are also consistent with this rationale. The secondary cracks form after the onset of necking, when a triaxial stress state develops and normal stresses begin to be exerted on the major grain boundary surfaces, especially near triple points and other areas of nonuniform stress. This was verified by sectioning specimens parallel to the load axis well after the onset of necking, but before fracture; no longitudinal cracks were found. Apparently the secondary cracks are formed immediately before or during final fracture.

The proposal that hydrogen embrittlement is at least a contributory process, and may be a dominant one, in the phenomenon of stress corrosion cracking (SCC) of 7Q75 and other high strength aluminum alloys has been presented by a number of investigators.[6,7,11,12,14,15,17,31,37,40-44] No direct evidence on this question is offered by the present results, but it is appropriate to consider the implications of this work for the SCC problem. Firstly, if there is a hydrogen embrittlement contribution to SCC in 7075, it need not occur solely through an effect on intergranular fracture; the present work demonstrates a distinct hydrogen effect on transgranular failure. Secondly, the fracture path appears to be a function of loading direction, with short transverse or RD-ST 45 deg specimens showing intergranular failures, and is not necessarily a function of electrochemical phenomena. This is consistent with the microstructural evidence in Speidel and Hyatt's review.[2] Thirdly, the decreasing sensitivity to hydrogen associated with increased aging is consistent with the parallel behavior of SCC susceptibility as a function of aging,[2] indicating at least the possibility that the SCC dependence on microstructure relates to hydrogen effects. This last point could be more directly investigated using Mode I-Mode III tests,[12] experiments which are now underway in our laboratory.

SUMMARY

The response of 7075 aluminum having three different microstructures (underaged, peak-aged and overaged) to cathodically charged hydrogen was examined in the test temperature range of −200 to 20°C. The principal results were:

1) For all microstructures, a temperature dependent loss of ductility due to hydrogen was found.

2) The effect was absent at the lowest test tempera-

ture, ruling out a purely mechanical effect due to charging damage present prior to mechanical testing.

3) The temperature dependence of the embrittling effect showed a distinct maximum, which was dependent on the microstructure; with increasing aging temperature, the maximum shifted towards lower test temperatures.

4) The ductility loss was a function of microstructure, being highest for the underaged and lowest for the overaged material, which suggests a correlation between hydrogen embrittlement and slip planarity. The pattern found here qualitatively mirrors the pattern found for stress corrosion cracking susceptibility.

5) It was found that the fracture mode was not affected by microstructure and charging condition. For all temperatures, a transgranular dimple type fracture was observed, which is believed to be due to test geometry relative to the pancake shaped grains. The dimple size data suggested enhancement of microvoid nucleation in T6 and T73 specimens, and enhancement of void growth in UT specimens, as the primary hydrogen effects.

All these results confirm a hydrogen embrittlement effect responsible for the ductility loss. However, more detailed experiments are needed to understand the fracture nucleation events as well as the hydrogen transport mechanism.

ACKNOWLEDGMENTS

We appreciate provision of the 7075 plate material by Alcoa Laboratories, through the efforts of E. H. Hollingsworth and the Alcoa Foundation; and experimental assistance from E. Danielson. This work was performed under the sponsorship of the Air Force Office of Scientific Research, Contract F49620-77-C-0003.

REFERENCES

1. A. Kelly and R. B. Nicholson: *Progr. Mater Sci.*, 1963, vol. 10, pp. 151-391.
2. M. O. Speidel and M. V. Hyatt: *Advances in Corrosion Science and Technology*, vol. 2, pp. 115-335, Plenum, NY, 1972.
3. M. W. Hyatt and M. O. Speidel: *Stress Corrosion Cracking in High Strength Steels and in Titanium and Aluminum Alloys*, pp. 147-244, Naval Res. Lab., Washington 1972.
4. R. H. Brown, D. O. Sprowls, and M. B. Shumaker: *Stress Corrosion Cracking of Metals - A State of the Art*, pp. 87-118, STP 518, ASTM, Philadelphia, 1972.
5. G. M. Ugiansky, L. P. Skolnick, and S. W. Stiefel: *Corrosion*, 1969, vol. 25, pp. 77-86.
6. A. W. Thompson and I. M. Bernstein: *Rev. Coat. Corros.*, 1975, vol. 2, pp. 3-44.
7. A. W. Thompson and I. M. Bernstein: *Advances in Corrosion Science and Technology*, vol. 7, pp. 53-175, Plenum, NY, 1979.
8. M. O. Speidel: *The Theory of Stress Corrosion Cracking in Alloys*, pp. 289-341, NATO., Brussels, 1971.
9. P. N. T. Unwin and R. B. Nicholson: *Acta Met.*, 1969, vol. 17, pp. 1379-93.
10. J. K. Tien, A. W. Thompson, I. M. Bernstein, and R. J. Richards: *Met. Trans. A*, 1976, vol. 7A, pp. 821-29.
11. M. O. Speidel: *Hydrogen in Metals*, pp. 249-73, ASM, Metals Park, OH, 1974.
12. J. A. S. Green, H. W. Hayden, and W. G. Montague: *Effect of Hydrogen on Behavior of Materials*, pp. 200-15, TMS-AIME, NY, 1976.
13. J. R. Low: *Progr. Mater. Sci.*, 1963, vol. 12, pp. 1-96.
14. W. E. Wood and W. W. Gerberich: *Met. Trans.*, 1974, vol. 5, pp. 1285-94.
15. A. W. Thompson: *Environmental Degradation of Engineering Materials*, pp. 3-17, VPI Press, Blacksburg, VA, 1977.
16. J. Albrecht, B. J. McTiernan, I. M. Bernstein, and A. W. Thompson: *Scr. Met.*, 1977, vol. 11, pp. 893-97.
17. R. J. Gest and A. R. Troiano: *L'Hydrogene dans les Metaux*, pp. 427-32, Éditions Science et Industrie, Paris, 1972.
18. R. J. Gest and A. R. Troiano: *Corrosion*, 1974, vol. 30, pp. 374-79.
19. A. W. Thompson: *Met. Trans.*, 1973, vol. 4, pp. 2819-25.
20. M. R. Louthan, G. R. Caskey, J. A. Donovan, and D. E. Rawl: *Mater. Sci. Eng.*, 1972, vol. 10, pp. 357-68.
21. A. W. Thompson: *Mater. Sci. Eng.*, 1974, vol. 14, pp. 253-64.
22. H. Y. Hunsicker: *Aluminum*, vol. 1, pp. 109-62 (esp. p. 154), ASM, Metals Park, OH, 1967.
23. *Metals Handbook*, vol. 8, 8th Ed., p. 31, ASM, Metals Park, OH, 1973.
24. A. R. Troiano: *Trans. ASM*, 1960, vol. 62, pp. 54-80.
25. J. Albrecht and G. Lütjering: *Influence of Microstructure on Fatigue Crack Propagation Rate of Aluminum Alloys*, Report ESA-TT-418, European Space Agency, Access No. N78-18203, DFVLR, Cologne, W. Germany, 1974.
26. L. M. Foster, T. H. Jack, and W. W. Hill: *Met. Trans.*, 1970, vol. 1, pp. 3117-24.
27. J. A. Donovan: *Met. Trans. A*, 1976, vol. 7A, pp. 1677-83.
28. M. R. Louthan, G. R. Caskey, and A. H. Dexter: *Radiation Effects and Tritium Technology for Fusion Reactors*, vol. IV, pp. 117-32, Oak Ridge Nat'l. Laboratory, Oak Ridge, TN, 1976.
29. H. W. Liu: *J. Basic Eng. (Trans. ASME, Series D)*, 1970, vol. 92D, pp. 633-38.
30. L. Montgrain and P. R. Swann: *Hydrogen in Metals*, pp. 575-84, ASM, Metals Park, OH, 1974.
31. G. M. Scamans, R. Alani, and P. R. Swann: *Corros. Sci.*, 1976, vol. 16, pp. 443-59.
32. G. M. Scamans: *J. Mater. Sci.*, 1978, vol. 13, pp. 27-36.
33. A. W. Thompson: *Effect of Hydrogen on Behavior of Materials*, pp. 467-77, TMS-AIME, NY, 1976.
34. A. W. Thompson: *Met. Trans. A*, 1979, vol. 10A, pp. 727-31.
35. G. S. Ansell, H. S. Kim, and H. C. Rogers: *Trans. ASM*, 1966, vol. 59, pp. 630-43.
36. A. W. Thompson and I. M. Bernstein: *Fracture 1977*, vol. 2, pp. 249-54, Univ. of Waterloo Press, Waterloo, Ontario, 1977.
37. R. J. Jacko and D. J. Duquette: *Met. Trans. A*, 1977, vol. 8A, pp. 1821-27.
38. P. Doig, P. E. J. Flewitt, and J. W. Edington: *Corrosion*, 1977, vol. 33, pp. 217-21.
39. J. M. Chen, T. S. Sun, R. K. Viswanadham, and J. A. S. Green: *Met. Trans. A*, 1977, vol. 8A, pp. 1935-40.
40. U. R. Evans: *Stress Corrosion Cracking and Embrittlement*, pp. 158-62, Wiley, NY, 1956.
41. J. C. Scully: *Effect of Hydrogen on Behavior of Materials*, pp. 129-47, TMS-AIME, NY, 1976.
42. R. M. Latanision, O. H. Gastine, and C. R. Compeau: *Environment-Sensitive Fracture of Engineering Materials*, pp. 48-70, TMS-AIME, Warrendale, PA, 1979.
43. A. J. Bursle and E. N. Pugh: *ibid.*, pp. 18-47.
44. A. W. Thompson: *ibid.*, pp. 379-410.